Tails of the crossing probability

Oleg A. Vasilyev*

Laboratoire de Physique Théorique de la Matière Condensée, Université Paris–VI, 75252 Paris Cedex 05, France and L. D. Landau Institute for Theoretical Physics RAS, 142432, Chernogolovka, Moscow region, Russia

(Received 6 April 2005; published 15 September 2005)

The scaling of the tails of the probability of a system to percolate only in the horizontal direction π_{hs} was investigated numerically for the correlated site-bond percolation model (q-state Potts model) for $q=1$, 2, 3, 4 (where q is the number of spin states). We have to demonstrate that the crossing probability $\pi_{hs}(p)$ far from the critical point p_c has the shape $\pi_{hs}(p)\simeq D\exp[cL(p-p_c)^{\nu}]$ where ν is the correlation length index, and $p=1-\exp(-\beta)$ is the probability of a bond to be closed. For the tail region the correlation length is smaller than the lattice size. At criticality the correlation length reaches the sample size and we observe crossover to another scaling $\pi_{hs}(p)\simeq A\exp\{-b[L(p-p_c)^{\nu}]^{x}\}$. Here x is a scaling index describing the central part of the crossing probability.

DOI: 10.1103/PhysRevE.72.036115 PACS number(s): 05.50.+q, 05.10.Ln, 64.60.Ak

I. INTRODUCTION

The scaling theory states that in the vicinity of the critical point for a system of linear size L the temperature critical behavior of thermodynamical quantities can be expressed as a function of a single variable $L^{1/\nu}(T-T_c)/T_c$ where T_c is the critical temperature and ν is the correlation length index [1]. The q-state Potts model can be represented as the correlated site-bond percolation in terms of Fortuin-Kasteleyn (FK) clusters [2]. At the critical point of the second order phase transition, an infinite cluster is formed. This cluster crosses the system connecting the opposite sides of the square lattice. There is a close relationship between percolation properties of FK clusters and critical properties of the Potts model. In the last decade the study of the shape of the crossing probability was performed by conformal methods [3–8] as well as numerically [9–18]. The continuum limit of the probability of a system to percolate in the horizontal direction $\pi_h(p_c)$ at the critical point p_c was investigated by Cardy by conformal field methods [3,4,8]. The analogous formula for the probability of a system to percolate in both directions $\pi_{hv}=\pi_h-\pi_{hs}$ was found by Watts [5]. The works of Smirnov [6,7] analytically proved that the crossing formula holds for the continuum limit of site percolation on the triangle lattice [6,7]. The conformal field method allows us to investigate crossing probabilities at the critical point for samples with different aspect ratio. The behavior of the crossing probability as a function of deviation from the critical point was investigated by numerical methods. Langlands *et al.* [9,10] show, that for site and bond percolation on square, honeycomb, and triangle lattices with the aspect ratios a, $a\sqrt{3}$, and $a\sqrt{3}/2$, respectively, the crossing probability π_h is the universal function of a. Hu, Lin, and Chen demonstrate that by choosing a very small number of nonuniversal metric factors, all scaled data for percolation functions and numbers of percolating clusters on square, honeycomb, and triangle lattices may fall on the same universal scaling functions [12–15]. They use the scaling variable $(p-p_c)L^{(1/\nu)}$, where p_c is the percolation critical point.

According to Refs. [19,20] the distribution function of the percolation thresholds is a Gaussian function. Following the number of works [11,17,18,21,22] the tails of the distribution function are not Gaussian and are described by a stretched exponent $\exp[C(p-p_c)^{\nu}]$. The authors of the recent work Ref. [23] are still uncertain about distinguishing a stretched exponential behavior from a Gaussian because no definitive conclusion can be extracted from their data.

The aim of this paper is to investigate the shape of the probability of a system to percolate only in the horizontal direction π_{hs}. We perform a numerical simulation of the correlated site-bond percolation model for $q=1$, 2, 3, 4 (the percolation model $q=1$, the Ising model $q=2$, and the Potts model $q=3$, 4) for lattice sizes $L=32$, 48, 64, 80, 128. The scaling formula for the body of the crossing probability at criticality $|\tau|\leq\tau_0$ and for tails of the crossing probability $|\tau|>\tau_0$ was obtained:

$$\pi_{hs}(\tau)=\begin{cases}A\exp(-b\tau^{x}), & |\tau|\leq\tau_0,\\ D\exp(-c\tau), & |\tau|>\tau_0,\end{cases} \tag{1}$$

where $\tau=L(p-p_c)^{\nu}$ is the scaling variable. The tails of the crossing probability on a finite lattice correspond to the critical region. In this critical region $|\tau|>\tau_0$ the correlation length ξ is smaller than the sample size $\xi<L$. As the temperature approaches the critical point τ_0, the correlation length reaches the sample size. In the region $|\tau|\leq\tau_0$ where the correlation length is greater than the sample size $\xi>L$, the function π_{hs} crosses over to the smoothed "body" part. This part is characterized by the index x. Two different scaling regions of the crossing probability indicate the uncertainty about the shape of this function.

The paper is organized as follows. In the second section, we describe details of the numerical simulation. In the third section, the method for determining the pseudocritical point $p_c(L,q)$ on the finite lattice is described. We use $p_c(L,q)$ to perform the approximation of the tails. In Sec. IV we approximate the double logarithm of the crossing probability

*Electronic address: vasilyev@itp.ac.ru

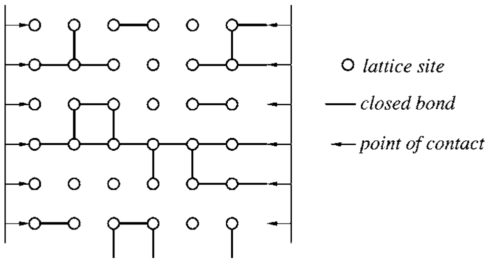

FIG. 1. The dual lattice with the horizontally spanning cluster.

$\ln\{-\ln[\pi_{hs}(p;L,q)]\}$ tails as a function of the logarithm of deviation from the critical point $\ln[p-p_c(L,q)]$ by the linear function $\tilde{c}(L,q)+y(L,q)\ln[p-p_c(L,q)]$ with slope y [$\tilde{c}(L,q)$ is a fitting parameter]. We obtain $y(L,q)\simeq\nu(q)$ for this approximation procedure. In Sec. V we describe a fitting procedure using the scaling variable $\tau=L(p-p_c)^{\nu}$. The results of the approximation are discussed in Sec. VI.

II. DETAILS OF NUMERICAL SIMULATION

We perform a massive Monte Carlo simulation on a square lattice of size L to obtain high-precision data for π_{hs}. We use the dual lattice shown in Fig. 1. On this lattice the critical point of the bond percolation ($q=1$) is exactly equal to $1/2$ and is not dependent on the lattice size [24]. To produce the pseudorandom numbers we use the R9689 random number generator with four taps [25]. We close each bond with a probability p and leave it open with a probability $1-p$. Then we split the lattice into clusters of connected sites by using the Hoshen-Kopelman algorithm [26]. After that we check the percolation through this configuration. We average the crossing probability over 10^7 random bond configurations.

We use the Wolff [27] cluster algorithm to generate a sequence of thermally equilibrated spin configurations for the Potts $q=2$, 3,4 model. For each particular inverse temperature $\beta=1/T$ we flip 20 000 Wolff clusters to equilibrate the system.

The deviation of the pseudocritical point on the finite lattice from the position of the critical point on the infinite lattice for the spin model is smaller for periodic boundary conditions (PBCs) rather than the open boundary conditions (OBCs) [28,29]. For this reason we use the PBCs for the Wolff algorithm. The Monte Carlo algorithm generates spin configurations on a torus. For a generated spin configuration we create a configuration of bonds. Each bond between sites with equal spin variable σ is closed with the probability $p=1-\exp(-\beta)$ and is open with probability $1-p=\exp(-\beta)$. Bonds between sites with different values of σ are always open in accordance with the Fortuin-Kasteleyn rule [2]. Then we split the particular spin and bond configurations into different clusters. Here we use OBCs. It means that for each generated configuration we cut the torus and check the crossing on the square with open boundary conditions. We fix the OBCs for crossing only in horizontal direction π_{hs} because it implies the vertical crossing is absent and the top and bottom rows must be disjointed. But we take into consideration the additional row and column of bonds, as shown in Fig. 1. In Fig. 1 contact points are shown by arrows. The left contact points are attached to the left column of sites. The right contact points are attached to additional bonds. In Fig. 1 the bond configuration with the horizontally spanning cluster is shown.

We check the percolation through an obtained cluster configuration, generate a new spin configuration, and so on. We average the crossing probability over 10^7 configurations for each value of the inverse temperature β. So the resolution of our computations is about 10^{-7}. In this way we perform a numerical simulation and get a set of data for $\pi_{hs}(p;L,q)$ for the lattice sizes $L=32$, 48, 64, 80, 128 and $q=2$, 3, 4. The formal definition of $\pi_{hs}(p;L,q)$ as a sum over different cluster configurations is described in [30].

For the Potts model we use the dual lattice as we do for the percolation. It means that we take into account additional bonds attached to the bottom row of spins. In the same way we take into account additional bonds attached to the right column of the spins. On the lattice with PBCs these bonds have to connect the right and the left columns. We cut the torus (because we use OBCs for the crossing probability) but we keep these additional bonds and take into account the checking of the crossing. Then we check the percolation through the obtained cluster configuration. After that we flip three Wolff clusters, check the spanning for a new spin configuration, and so on.

III. DETERMINATION OF THE PSEUDOCRITICAL POINT ON THE FINITE LATTICE

We investigate the crossing probability as a function of deviation from the critical point. Therefore, we perform preliminary approximations to obtain the critical points for the finite samples; namely, we obtain the pseudocritical point and the shape of the central part of the crossing probability, determine the shape of the tails of the crossing probability, combine together the information for body and tails, and reconstruct the total shape of the crossing probability.

We need to recall that we consider the crossing probability as a function of the variable $p=1-\exp(-\beta)$ (probability of a bond to be closed). It is easy to understand that we must take the pseudocritical point on the finite lattice $p_c(L,q)$ as the reference point. The crossing probability is a symmetric function of the variable $\Delta p=[p-p_c(L,q)]$. This fact implies that the high-temperature tail $p_c-\Delta p$ ($\Delta p>0$) and the low-temperature tail $p_c+\Delta p$ coincide $\pi_{hs}(p_c-\Delta p)=\pi_{hs}(p_c+\Delta p)$. For the bond percolation on the dual lattice the position of the percolation point does not depend on the lattice size $p_c(L,q=1)=0.5$ [24].

To determine the Ising and the Potts model critical point $p_c(L,q)$ we use the following procedure. We can assume [30] that in the region $-6<\ln[\pi_{hs}(p;L,q)]$ the following fitting formula is true:

$$F(p;L,q)=A(q,L)\exp(-\{B(L,q)[p-p_c(L,q)]\}^{\zeta(L,q)}). \tag{2}$$

Here $A(L,q)$ defines the crossing probability in the critical point, $B(L,q)$ is a scaling variable, $p_c(L,q)$ is the position of the pseudocritical point on the lattice L, and $\zeta(L,q)$ is a scaling index. Therefore we fit the logarithm of the crossing probability $\ln(\pi_{hs})$ by the function $f_1(p;L,q) = \ln[F(p;L,q)]$, namely,

$$f_1(p;L,q) = a(L,q) - \{B(L,q)[p - p_c(L,q)]\}^{\zeta(L,q)}, \qquad (3)$$

where $a(L,q) = \ln[A(L,q)]$.

We plot the data for $\ln[\pi_{hs}(p;L,q)]$ as a function of p in Figs. 2(a)–2(d) for $q=1$, 2, 3, and 4, respectively. The error bars in these figures are about the symbol size. It seems that the behavior of $\ln[\pi_{hs}(p;L,q)]$ near p_c is parabolic. The results of the approximation are plotted in the same figures by lines. We shall see that there is a good agreement between the numerical data and the results of the approximation. But we see deviation at the point p_c especially for $q=3$, 4. In the vicinity of p_c real graphs are smoother than fitting functions. Finally for each pair of numbers (L,q) we obtain four fitting parameters $A(L,q)$, $B(L,q)$, $p_c(L,q)$, and $\zeta(L,q)$.

The fitting parameter $a(L,q) = \ln[A(L,q)]$ defines a vertical shift of graphs from the zero level in Figs. 2(a)–2(d). We approximate the data for $B(L,q)$ by the function $b^*(L,q)L^{u(L,q)}$.

In Fig. 3(a) the results of the approximation are plotted by lines. The values of the fitting parameters $b^*(L,q)$ and $u(L,b)$ as well as the inverse correlation length index $1/\nu$ are placed in Table I. We can see for $q=1$, 2, 3 that $u(L,q) \simeq 1/\nu(q)$. It can be assumed that

$$B(L,q) = b^*(L,q)L^{1/\nu(q)}. \qquad (4)$$

In the case $q=4$ the scaling index $u(q)$ is not equal $1/\nu(q=4)$. Many critical quantities in the Potts model $q=4$ exhibit logarithmic corrections [31–34]. These logarithmic corrections explain the difference between the analytical value $1/\nu(q=4)=1.5$ and the numerical approximation for the scaling index $u=1.372(8)$.

The critical point in the p scale for the q-state Potts model on the infinite lattice is $p_c^{\text{precise}} = \sqrt{q}/(1+\sqrt{q})$ (see Ref. [35]). The numerical results for the position of the critical point for the finite lattices as a function of the lattice size L are shown in Fig. 3(b). On the dual lattice the position of the critical point for percolation is equal to $\frac{1}{2}$ and does not depend on the lattice size. For our computation for all points $p_c(L,q)$ the deviations from 0.5 are less than 0.0001. This deviation corresponds to the numerical inaccuracy of our Monte Carlo simulation.

The data $p_c(L,q)$ for $q=2$, 3, 4 were approximated by a power function of the lattice size $p_c(L,q) \simeq p_c(q) + dp(q)L^{v(q)}$. The results of the approximation are placed in Table II and are also plotted by lines in Fig. 3(b). We shall see that our fitting procedure determines the critical point with accuracy up to four digits after the decimal point. Thus, we shall use the obtained values $p_c(L,q)$ for the following approximation of the tails of the crossing probability. In Table III we place the results of the approximation for the index $\zeta(L,q)$ describing the curvature of the central part of the crossing probability.

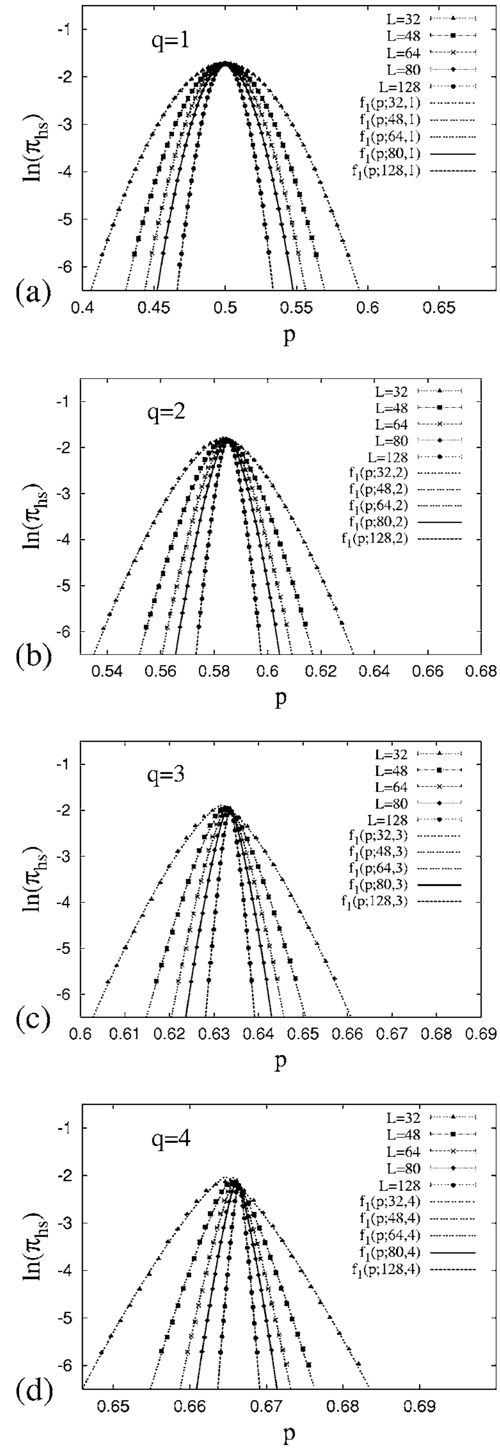

FIG. 2. Approximation of the logarithm of the crossing probability $\ln(\pi_{hs})$ as a function of p by the function $f_1(p;L,q) = a(L,q) - \{B(L,q)[p-p_c(L,q)]\}^{\zeta(L,q)}$, for (a) percolation $q=1$; (b) Ising model $q=2$; (c) Potts model $q=3$; (d) Potts model $q=4$.

IV. THE SHAPE OF THE CROSSING PROBABILITY π_{hs} TAILS: DIRECT APPROACH

Let us check the shape of the crossing probability tails. The double logarithm of the crossing probability $\ln\{-\ln[\pi_{hs}(L,q)]\}$ are plotted as functions of the variable t

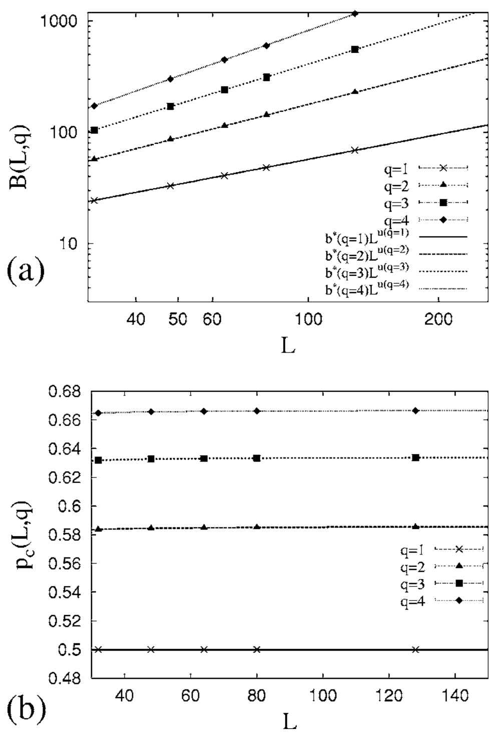

FIG. 3. (a) The fitting parameter $B(L,q)$ as a function of L. Results of the approximation by functions $b^*(L,q)L^{u(L,q)}$ (see Table I) are plotted by lines. (b) Position of the pseudocritical point on the finite lattice $p_c(L,q)$ as a function of the lattice size L for $q=1$, 2, 3, 4 and approximation by the power law $p_c(L,q)=p_c(\infty,q)+dp(q)L^{v(q)}$ for $q=2$, 3, 4. Line 0.5 is also added.

$=\ln[|p-p_c(L,q)|]$ in Figs. 4(a)–4(d) for $q=1$, 2, 3, and 4, respectively.

The points for high-temperature and low-temperature tails lie on the same lines. This again validates our fitting procedure.

We expect that the crossing probability tails are described by the formula

$$\pi_{hs}(p;L,q) = D(L,q)\exp\{-C(L,q)[p-p_c(L,q)]^{y(L,q)}\}. \tag{5}$$

Here $D(L,q)$ is the prefactor, $p_c(L,q)$ is the position of the pseudocritical point, and the variables $C(L,q)$ and $y(L,q)$ define the shape of tails. In the interval $\ln(6) \leqslant \ln\{-\ln[\pi_{hs}(L,q)]\} \leqslant \ln(12)$ the tails of the crossing probability look like straight lines.

The absence of a prefactor before the exponent in Eq. (5) was argued in Ref. [18] for the case of wrapping in the horizontal direction in terms of the transfer matrix. We cannot directly apply the same arguments in our case, because we consider another function—the probability of crossing only in the horizontal direction. The presence of a prefactor must cause the deviation from linear dependence in Fig. 4 in accordance with Eq. (6):

$$\ln[-\ln(\pi_{hs})] = \ln\{-d(L,q) + C(L,q)\exp[ty(L,q)]\} \simeq \ln[C(L,q)] + y(L,q)t - \frac{d(L,q)}{C(L,q)\exp[ty(L,q)]}. \tag{6}$$

Here $d(L,q)=\ln[D(L,q)]$ and $t=\ln[|p-p_c(L,q)|]$ the logarithms of deviation from the critical point. But deviation due to the prefactor $D(L,q)\neq 1$ exponentially decreases as t grows so it is possible to avoid the deviation from the linear dependence by appropriate choice of an interval of approximation. In the region of approximation points in Fig. 4 lie on the lines with good accuracy. We obtain the set of $p_c(L,q)$ for $L=32, \ldots, 128$ and $q=2$, 3, 4 in Sec. III. Using these data let us approximate the double logarithm of the tails $\ln[-\ln(\pi_{hs})]$ as a function of t by the formula (7)

$$f_2(t;L,q) = \tilde{c}(L,q) + y(L,q)t. \tag{7}$$

Combining Eqs. (5) and (7), we obtain $\tilde{c}(L,q)=\ln[C(L,q)]$. The resolution of our computations 10^{-7} is about 16 units on the $(-\ln)$ scale and is about 2.7 units on the $[\ln(-\ln)]$ scale. We use the points in the interval $\ln(6) < \ln[-\ln(\pi_{hs})] < \ln(12)$, $\ln(6)\simeq 1.79, \ln(12)\simeq 2.48$, for this approximation. This interval is indicated in Figs. 4(a)–4(d) by horizontal lines. In this figures the slope lines represent results of approximation for $y(L,q)$.

In the region $\ln[-\ln(\pi_{hs}])<\ln(6)$ the crossing probability obeys another scaling formula. In the region $\ln[-\ln(\pi_{hs})] > \ln(12)$ the numerical inaccuracy becomes large. There are only a few numbers of "hits" in horizontally spanning clus-

TABLE I. Data for fitting parameters $b^*(L,q)$, $u(L,q)$.

L	$q=1$	$q=2$	$q=3$	$q=4$
$b^*(L,q)$	1.84(2)	1.767(9)	1.63(2)	1.49(5)
$u(L,q)$	0.746(3)	1.002(1)	1.198(4)	1.372(8)
$1/\nu(q)$	0.75	1	1.2	1.5

TABLE II. Results of approximation of $p_c(L,q)$ by the power law $p_c(q)+dp(q)L^{v(q)}$. The analytical values $p_c^{\text{precise}}(q)=\sqrt{q}/(\sqrt{q}+1)$ are added for comparison.

q	$dp(q)$	$v(q)$	$p_c(q)$	$p_c^{\text{precise}}(q)$
2	−0.160(5)	−1.25(1)	0.58573(2)	0.585786…
3	−0.22(2)	−1.33(2)	0.63394(2)	0.633975…
4	−0.26(2)	−1.42(4)	0.66666(1)	0.6666666…

TABLE III. Results of the approximation for $\zeta(L,q)$.

L	$q=1$	$q=2$	$q=3$	$q=4$
32	1.887(6)	1.52(2)	1.38(3)	1.28(3)
48	1.883(7)	1.52(2)	1.37(3)	1.27(3)
64	1.882(6)	1.52(2)	1.38(3)	1.28(3)
80	1.885(7)	1.52(2)	1.38(3)	1.30(3)
128	1.86(1)	1.52(2)	1.37(3)	1.28(3)

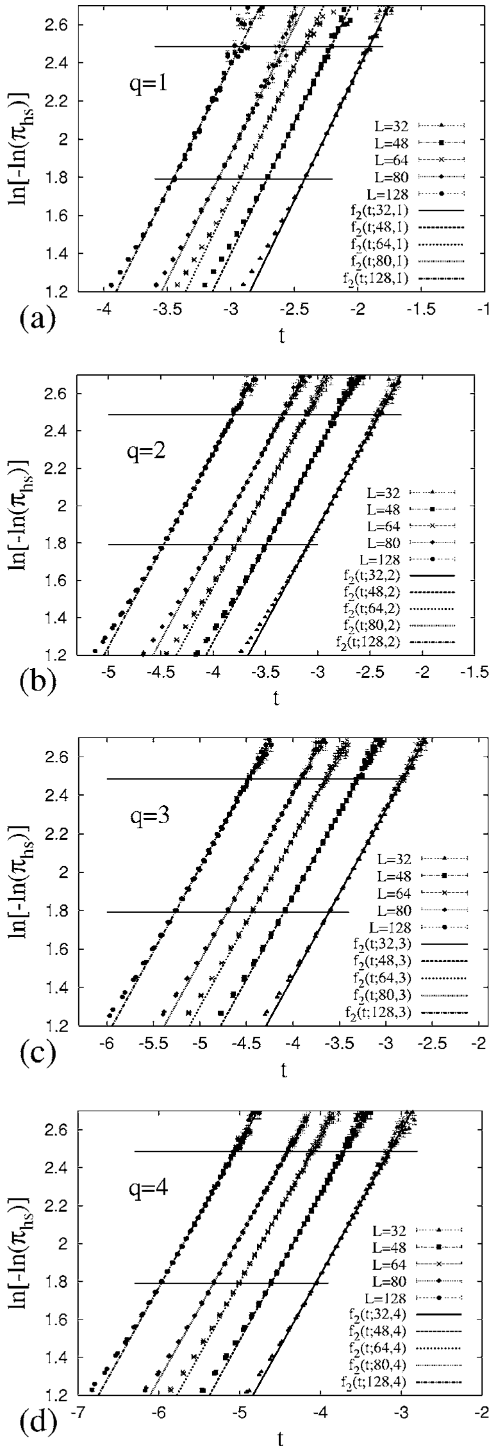

FIG. 4. Approximation of the double logarithm of the crossing probabilities $\ln\{-\ln[\pi_{hs}(p;L,q)]\}$ by the function $f_2(t;L,q)$ $=\tilde{c}(L,q)+y(L,q)t$ of the logarithm of the distance to the critical point $t=\ln[|p-p_c(L,q)|]$ for (a) percolation $q=1$; (b) Ising model $q=2$; (c) Potts model $q=3$; (d) Potts model $q=4$. The range of the approximation region is shown by horizontal lines.

ters for $\ln[-\ln(\pi_{hs})]>\ln(12)$. Results of the numerical approximation for $y(L,q)$ are presented in Table IV.

As we can see $y(L,q)\simeq\nu(q)$. The exception is the case $q=4$. For $q=4$ we obtain $y(L,q=4)\simeq 3/4$ instead of $\nu(q=4)=2/3$. This deviation can be explained by the logarithmic corrections. Some deviations exceeding the approximation errors can be explained by the choice of the approximation region. As can be seen from Figs. 4(a)–4(d) decreasing of the bottom approximation range ln(6) causes decreasing of the slope of the approximation line. From all said above we can conclude that the tails of the crossing probability behave like $\exp[-(p-p_c)^\nu]$.

We fit the parameter $\tilde{c}(L,q)$ by the expression $c_1^*+c_2^*\ln(L)$. In Fig. 5 the fitting parameter $\tilde{c}(L,q)$ is plotted as a function of L for $q=1$, 2, 3, 4 as well as the results of the approximation $c_1^*+c_2^*\ln(L)$.

The parameter c_2^* for all q is equal to 1 within accuracy of the approximation. In accordance with scaling theory for the system of size L the deviation from the critical point is described by the expression $L(p-p_c)^\nu$. Therefore we may assume that

$$\pi_{hs}(p;L,q) \simeq D(L,q)\exp\{-c(q)L[p-p_c(L,q)]^{\nu(q)}\}. \quad (8)$$

V. MODIFIED FITTING PROCEDURE

From the above we can make the following conclusions. There are two scaling regions: the first one is in the vicinity of the critical point, and the second is in the tails. Analyzing Eqs. (2), (4), and (8) we can conclude that the distance from the critical point $[p-p_c(L,q)]$ and the lattice size L occur in a formula only as the combination $L/\xi\sim L[p-p_c(L,q)]^{\nu(q)}$ in accordance with scaling theory. Let us introduce the scaling variable

$$\tau = L[p-p_c(L,q)]^{\nu(q)}. \quad (9)$$

If we plot the negative logarithm of the crossing probability $-\ln(\pi_{hs})$ as a function of the scaling variable τ then we expect power dependence in the vicinity of zero and linear dependence for the tails. We can use the scaling variable $\tau=L[p-p_c(L,q)]^{\nu(q)}$ to fit the crossing probability taking into account the finite size scaling. Let us describe our fitting procedure.

We may assume that we obtain the position of the critical point on the finite lattice $p_c(L,q)$ as a result of the previous fit. Thus, we can use only three free fitting parameters and fix the value $p_c(L,q)$. Substituting Eq. (9) for τ in Eqs. (3) and (5), we obtain the fitting formulas for the body and the tails of the crossing probability:

$$-\ln(\pi_{hs}) \simeq f_3(\tau;L,q) = -a(L,q)+b(L,q)\tau^{x(L,q)}, \quad (10)$$

$$-\ln(\pi_{hs}) \simeq f_4(\tau;L,q) = -d(L,q)+c(L,q)\tau. \quad (11)$$

Here $\tau=L[p-p_c(L,q)]^{\nu(q)}$ and a,d,c,x are fitting parameters.

The numerical value of the variable $p_c(L,q)$ is used for computation of τ in accordance with Eq. (9). Comparing the fitting procedures Eqs. (10) and (11) and the previous fitting procedures Eqs. (3) and (5) we can obtain relations between the fitting parameters $b(L,q)$, $x(L,q)$, $c(L,q)$ and the parameters $b^*(L,q)$, $\zeta(L,q)$, $C(L,q)$:

$$b(L,q) = b^*(L,q)^{\zeta(q)}, \quad (12)$$

TABLE IV. The slopes of lines, results of the approximation for $y(L,q)$; the analytical values $\nu(q)$ are presented for comparison.

L	$q=1$	$q=2$	$q=3$	$q=4$
	$4/3 \simeq 1.3333$	1	$5/6 \simeq 0.83333$	$2/3 \simeq 0.6666$
32	1.366(11)	1.026(23)	0.87(2)	0.761(21)
48	1.375(10)	1.030(12)	0.868(12)	0.772(14)
64	1.376(12)	1.035(8)	0.877(8)	0.767(10)
80	1.32(3)	1.032(10)	0.872(13)	0.752(14)
128	1.31(4)	1.036(5)	0.874(6)	0.759(4)

$$\zeta(L,q) = x(L,q)\,\nu(L,q), \tag{13}$$

$$C(L,q) = c(L,q)L,\ \tilde{c}(L,q) = \ln[C(L,q)]. \tag{14}$$

The special case is $q=4$. As we can observe from the results of the approximations in Tables I and IV the finite size scaling of the crossing probability for $q=4$ does not obey the scaling law $L(p-p_c)^{\nu(q=4)}$ (probably due to logarithmic corrections to scaling). Therefore, instead of the analytical value $\nu(q=4)=2/3$ we use the numerical approximation $y(q=4)=3/4$ from Table IV. We will see later that this substitution allows us to obtain correct results for the scaling.

We perform the fitting procedure in accordance with the formulas proposed above. For the fit of the body of the crossing probability Eq. (10) the scaling region $1.6 < -\ln(\pi_{hs}) < 6$ was used. For the fit of the tails of the crossing probability Eq. (11) we use the scaling region $6 < -\ln(\pi_{hs}) < 12$.

We place the results of the fitting procedure for $q=1$, 2, 3, and 4 in Figs. 6(a)–6(d), respectively. In these figures the fitting region is denoted by horizontal lines. As we expect, if we plot the data as functions of the scaling variable τ then the finite size dependence is eliminated and the points for different values of L lie on the same curves. The results of the approximation for $b(L,q)$, $c(L,q)$, and $d(L,q)$ demonstrate that these fitting parameters do not depend on the lattice size L. The absolute value of the parameter $d(q)$ is relatively small so the prefactor $D(q)$ is about 1. For percolation the order of $d(q=1)$ is less than three times the value of the numerical inaccuracy; thus it is possible that $d(q=1)=0$. All dependence on L is enclosed in the expression for τ. Hence we can omit the variable L in the parentheses and consider $b(q)$ only as a function of q. This fact validates the choice of the fitting procedure.

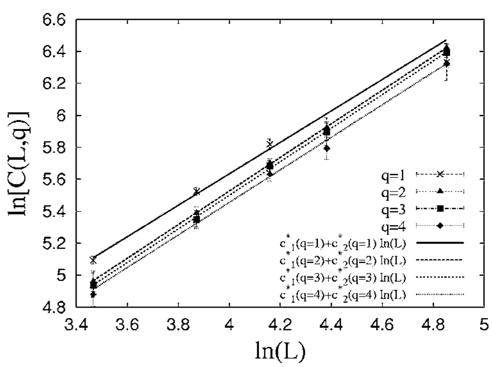

FIG. 5. The fitting parameter $\tilde{c}(L,q)=\ln[C(L,q)]$ (the vertical shift of the approximation lines for tails) as a function of $\ln(L)$ for $q=1$, 2, 3, 4. Results of approximation $c_1^*(q)+c_2^*(q)\ln(L)$ are shown by lines.

The data in Table V presents some power $x(q)$. This power describes the behavior of the crossing probability in the vicinity of the critical point as a function of the scaling variable τ and does not depend on the lattice size.

VI. DISCUSSION

Using the dual lattice (see Fig. 1) allows us to avoid a finite size shift of the critical point for the bond percolation and to diminish it for spin models. The accuracy of definition of the critical point on the finite lattice plays a principal role for the investigation of the tail scaling. The high quality of our approximation is proved by the remarkable symmetry of the crossing probability with respect to the critical point p_c. In Figs. 4 and 6 we can observe that the two branches $p-p_c>0$ and $p-p_c<0$ practically coincide.

Let us discuss the meaning of the two scaling regions of the crossing probability. In Fig. 7(a) we plot the crossing probability by crosses (bottom) and the magnetic susceptibility χ by triangles (top) for the Ising model ($q=2$) on the lattice $L=128$ as functions of the inverse temperature β with a logarithmic scale for the ordinate axis.

In Fig. 7(b) we plot (by crosses) the same data for the crossing probability as a function of the absolute value of the scaling variable $\tau=L(p-p_c)^{\nu}$ where $p=1-\exp(-\beta)$. In Fig. 7(b) the position of the crossover region of the crossing probability is indicated by solid horizontal line. In Fig. 7(a) we also indicate the position of the crossover region of π_{hs} by horizontal solid line on the same level as well as in Fig. 7(b). For the magnetic susceptibility we mark by horizontal dashed lines the region with critical behavior

$$\chi(\beta) \sim [(\beta-\beta_c)/\beta_c]^{-\gamma}, \tag{15}$$

where γ is the critical index of the magnetic susceptibility. We see from Fig. 7(a) that the tails of the crossing probability directly correspond to the critical region of the magnetic susceptibility. In this critical region the correlation length ξ is smaller than the sample size $\xi < L$. As the temperature approaches the critical point, the correlation length reaches the sample size. At that point the magnetic susceptibility on the

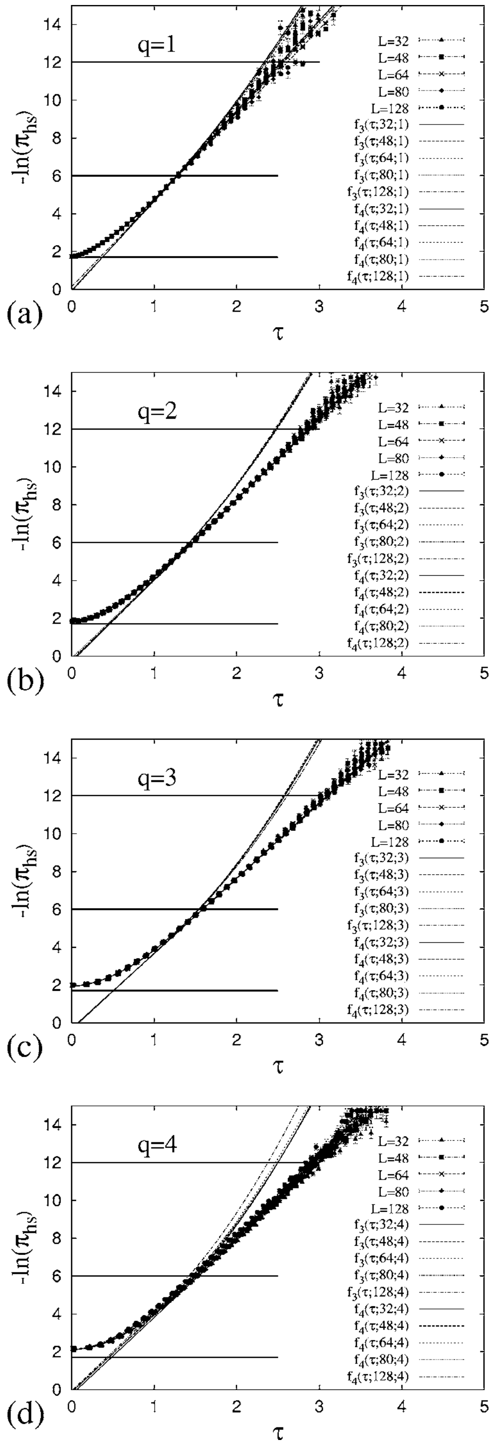

FIG. 6. The negative logarithm of the crossing probability $-\ln[\pi_{hs}(p;L,q)]$ as a function of the scaling variable $\tau=L[p-p_c(L,q)]^{\nu(q)}$ for (a) percolation $q=1$; (b) Ising model $q=2$; (c) Potts model $q=3$; (d) Potts model $q=4$. Results of the approximation of the body of the crossing probability by the function $f_3(\tau;L,q)=-a(L,q)+b(L,q)\tau^x$ and tails of the crossing probability by the function $f_4(\tau;L,q)=-d(L,q)+c(L,q)\tau$ are added. The ranges of the approximation regions are shown by horizontal lines.

finite lattice deviates from the critical behavior Eq. (15) and becomes smooth—see the region over the top dashed horizontal line in Fig. 7(a). At the same point the crossing probability crosses over from tails to body—the region over the solid horizontal line in Fig. 7(a) [and the region *under* the horizontal line in Fig. 7(b)]. At the critical point $\beta_c=-\ln(1-p_c)\simeq 0.881\,373\ldots$ both the magnetic susceptibility and the crossing probability reach a maximum. We can see from Fig. 7(b) that the function $\pi_{hs}(\tau)$ consists of two parts: the body $|\tau|<\tau_0$ and the tails $|\tau|>\tau_0$. The negative logarithm of the body of the crossing probability as a function of τ is well described by the function $-\ln[A(q)]+b(q)|\tau|^{x(q)}$ [the solid line on Fig. 7(b)]. The negative logarithm of the tails of the crossing probability have shape $-\ln[D(q)]+c(q)\tau$ [the dashed line in Fig. 7(b)]. This line is tangent to the body at the point $\tau_0(q)$; namely, this point is marked by the horizontal line. The two different scaling regions of the crossing probability clearly seen in Fig. 7(b) can explain the long time uncertainty about its shape. In Ref. [20] the scaling index for

TABLE V. Results of the approximation for the fitting parameter $x(L,q)$.

L	$q=1$	$q=2$	$q=3$	$q=4$
32	1.432(3)	1.61(2)	1.75(3)	1.82(3)
48	1.426(4)	1.59(2)	1.77(3)	1.78(3)
64	1.413(5)	1.59(2)	1.76(4)	1.78(4)
80	1.432(4)	1.60(3)	1.73(4)	1.73(3)
128	1.432(6)	1.61(3)	1.74(4)	1.81(5)

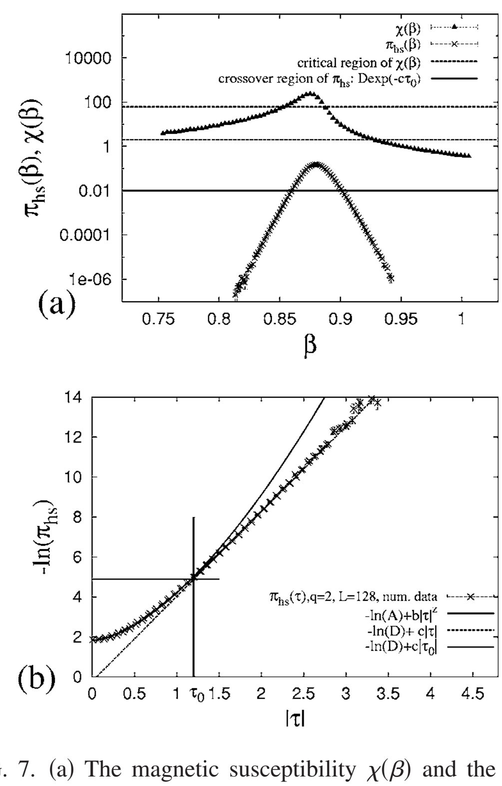

FIG. 7. (a) The magnetic susceptibility $\chi(\beta)$ and the crossing probability $\pi_{hs}(\beta)$ as functions of the inverse temperature β for the Ising model, $L=128$. (b) The negative value of the logarithm of the crossing probability $-\ln(\pi_{hs})$ for the Ising model as a function of the absolute value of the scaling variable $\tau=L(p-p_c)^{\nu}$ on the lattice $L=128$.

the percolation threshold for the two-dimensional percolation model was found to be $\zeta \simeq 1.9(1)$. This result coincides with our approximation of the body of the crossing probability for percolation, $\zeta \simeq 1.864(12)$. In more recent work [11,17,18,21,22] the tail region for percolation was investigated, which is described by the scaling formula $D(q)\exp[-c(q)L(p-p_c)^{\nu=4/3}]$. The crossover form to Gaussian-like behavior to slope 4/3 is observed in figures of Ref. [23]. It seems, near the critical point, that the behavior of the crossing probability is parabolic. The rounding happens in the interval $\tau < 0.1$. This interval is relatively small in comparison with regions of the body $0.1 < |\tau| < 1.5$ and tails $1.5 < |\tau| < 4$ as can be seen in Figs. 6 and 7(b).

We have five fitting parameters $a(q)$, $b(q)$, $x(q)$, $c(q)$, and $d(q)$ in expressions (10) and (11). In Figs. 6(a)–6(d) we see the crossover region between the body and the tails of the crossing probability. In this region the function f_3 touches the line f_4. This means that at some point $\tau_0(q)$ the values of the functions are equal; therefore

$$-a(L,q) + b(q)[\tau_0(q)]^{x(q)} = -d(L,q) + c(q)\tau_0(q), \quad (16)$$

and the first derivatives of these functions are equal too,

$$x(q)b(q)[\tau_0(q)]^{x(q)-1} = c(q). \quad (17)$$

Substituting $c(q)$ from Eq. (17) in Eq. (16) we obtain the expression for $b(q)$,

$$b(q) = \frac{d(q) - a(q)}{[x(q) - 1][\tau_0(q)]^{x(q)}}. \quad (18)$$

If the crossing probabilities at the critical points $A(q)$ [and logarithms $a(q)$] can be calculated analytically by conformal field methods (at least for the percolation it is possible) [3–5] then only four independent parameters $b(q)$, $\tau_0(q)$ and $x(q)$, $a(q)$ remain for the crossing probability. In such a way we propose the approximation formula for the crossing probability π_{hs}. The crossing probability as a function of the variable $\tau = L(p-p_c)^{\nu}$ consists of two parts:

$$\pi_{hs}(\tau,q) = \begin{cases} A(q)\exp[-b(q)\tau^{x(q)}], & |\tau| \leq \tau_0(q), \\ D(q)\exp[-c(q)\tau], & |\tau| > \tau_0(q), \end{cases} \quad (19)$$

where the parameters are connected by Eqs. (17) and (18). The main statements for the crossing probability π_{hs} are as follows.

(1) In accordance with scaling theory the finite size scaling of the crossing probabilities may be eliminated by introducing the scaling variable $\tau = L[p-p_c(L,q)]^{\nu(q)}$. The crossing probability as a function of τ does not depend on the lattice size L.

(2) The body of the crossing probability scales as $\pi_{hs}(\tau) \simeq A(q)\exp[-b(q)\tau^{x(q)}]$.

(3) The tails of the crossing probabilities scale as $\pi_{hs}(\tau) \simeq D(q)\exp[-c(q)\tau]$.

(4) The finite size scaling for $q=4$ is not described by the analytical value of the correlation length index $\nu(q=4) = 2/3$. We obtain a scaling index $y(q=4) \simeq 0.759(4)$ for the tails of the crossing probability (see Table IV) or $1/u(q) \simeq 0.728$ for the body of the crossing probability (see Table I).

ACKNOWLEDGMENTS

The author would like to thank Robert M. Ziff for helpful discussions and Théa Bellou for reading the manuscript and for her remarks.

[1] R. B. Stinchcombe, in *Phase Transitions and Critical Phenomena*, edited by C. Domb and J. L. Lebowitz (Academic, New York, 1983), Vol. 7.
[2] C. M. Fortuin and P. M. Kasteleyn, Physica (Amsterdam) **57**, 536 (1972).
[3] J. L. Cardy, Nucl. Phys. B **275**, 200 (1986).
[4] J. L. Cardy, J. Phys. A **25**, L201 (1992).
[5] G. M. T. Watts, J. Phys. A **29**, L363 (1996).
[6] S. Smirnov and W. Werner, Math. Res. Lett. **8**, 729 (2001).
[7] S. Smirnov, C. R. Acad. Sci., Ser. I: Math. **333**, 239 (2001).
[8] J. L. Cardy, eprint cond-mat/0209638.
[9] R. P. Langlands, C. Pichet, P. Pouliot, and Y. Saint-Aubin, J. Stat. Phys. **67**, 533 (1992).
[10] R. P. Langlands, Ph. Pouliot, and Y. Saint-Aubin, Bull., New Ser., Am. Math. Soc. **30**, 1 (1994).
[11] R. M. Ziff, Phys. Rev. Lett. **72**, 1942 (1994).
[12] Ch.-K. Hu, C.-Yu Lin, and J.-A. Chen, Phys. Rev. Lett. **75**, 193 (1995).
[13] Ch.-K. Hu and Chai-Yu Lin, Phys. Rev. Lett. **77**, 8 (1996).
[14] C.-Yu Lin and Ch.-K. Hu, Phys. Rev. E **58**, 1521 (1998).
[15] C.-K. Hu, J.-A. Chen, and C.-Y. Lin, Physica A **266**, 27 (1999).
[16] R. P. Langlands, M.-A. Lewis, and Y. Saint-Aubin, J. Stat. Phys. **98**, 131 (2000).
[17] M. E. J. Newman and R. M. Ziff, Phys. Rev. Lett. **85**, 4104 (2000).
[18] M. E. J. Newman and R. M. Ziff, Phys. Rev. E **64**, 016706 (2001).
[19] M. E. Levinshtein, B. I. Shklovskii, M. S. Shur, and A. L. Efros, Sov. Phys. JETP **42**, 197 (1976).
[20] F. Wester, Int. J. Mod. Phys. C **11**, 843 (2000).
[21] J. Berlyand and J. Wehr, J. Phys. A **28**, 7127 (1995).
[22] J.-P. Hovi and A. Aharony, Phys. Rev. E **53**, 235 (1996).
[23] P. M. C. de Oliveira, R. A. Nobrega, and D. Stauffer, J. Phys. A **37**, 3743 (2004).
[24] R. M. Ziff and M. E. J. Newman, Phys. Rev. E **66**, 016129 (2002).
[25] R. M. Ziff, Comput. Phys. **12**, 385 (1998).
[26] J. Hoshen and R. Kopelman, Phys. Rev. B **14**, 3438 (1976).
[27] U. Wolff, Phys. Rev. Lett. **62**, 361 (1988).
[28] D. P. Landau, Phys. Rev. B **13**, 2997 (1976).
[29] D. P. Landau, Phys. Rev. B **14**, 255 (1976).
[30] O. A. Vasilyev, Phys. Rev. E **68**, 026125 (2003).
[31] J. L. Cardy, M. Nauenberg, and D. J. Scalapino, Phys. Rev. B **22**, 2560 (1980).
[32] J. Salas and A. D. Sokal, J. Stat. Phys. **92**, 729 (1998).
[33] J. Asikainen *et al.*, Eur. Phys. J. B **34**, 479 (2003).
[34] J. Cardy and R. Ziff, J. Stat. Phys. **110**, 1 (2003).
[35] R. J. Baxter, *Exactly Solved Models in Statistical Mechanics* (Academic Press, New York, 1982).